



Università degli Studi di Padova

DIPARTIMENTO DI MATEMATICA

Corso di Laurea in Matematica

TESI DI LAUREA TRIENNALE

**On the detection
of the linear stability region
for L_4 and L_5 in the
Elliptic Restricted Three-Body Problem**

Laureando:

Gianmarco Tosatto

Relatore:

Prof. Francesco Fassó

Anno Accademico 2011-2012

Contents

| | |
|---|-----------|
| Introduction | 5 |
| 1 Hamiltonian formulation | 7 |
| 1.1 Hamiltonian function | 7 |
| 1.1.1 Hamiltonian vector field | 9 |
| 1.2 Extended phase space | 10 |
| 1.3 Hamiltonian vector field with E-property | 11 |
| 2 Bounding the stability region | 15 |
| 2.1 Separation of the fourth-order system | 15 |
| 2.2 Transition curves | 18 |
| 3 Numerical results | 21 |
| 3.1 Algorithms | 21 |
| 3.2 Stability region in the μ - e plane | 22 |
| 3.2.1 Numerical and analytical boundaries | 23 |
| 3.2.2 Right limit point | 24 |
| 3.3 Reduced integration | 25 |

Introduction

In this thesis we treat the linear stability of equilibrium points L_4 and L_5 in the Elliptic Restricted Three-Body Problem. The purpose of our work is to present and compare different approaches to this problem, and the steps that we have chosen to make can be summarized as follows.

In the first chapter we present a Hamiltonian formulation of the problem and we use the Poincaré-Lyapunov theory to present some classical results on linear stability on the parameter plane. Then we define an interesting property for systems of differential equations, introduced by Hale in [3], and we show how to take advantage of that in our problem, retracing what has been done by Meire and Vanderbauwhede in [6].

In the second chapter we present a lesser-known theory developed by Tschauner in [9], which allows to reduce the order of the differential systems used so far. Then we explain the notion of *transition curve* and we discuss how Meire in [5] proposes to search for the boundaries of the linear stability region.

In the third chapter we discuss some numerical results, comparing them with those obtained by Danby, [2], and Meire, [5].

Chapter 1

Hamiltonian formulation

Let us consider two bodies that revolve around their center of mass in elliptic orbits under the influence of their mutual gravitational attraction and a third body (attracted by the previous two but not influencing their motion) that moves in the plane defined by the two revolving bodies: the Elliptic Restricted Three-Body Problem is to describe the motion of this third body. Note that this is an approximation of the Three-Body Problem that still results not integrable.

In the Nechville coordinate system, in which the two revolving bodies result to be in quiet, the Lagrangian function of the ERTBP is

$$L(q, \dot{q}, t) = \frac{1}{2} r^2(t) \|\dot{q}\|^2 + c \sqrt{GM} q \cdot \mathbb{E}_2 \dot{q} + \frac{GM}{r(t)} (V(q) + \frac{1}{2} \|q\|^2) \quad (1.1)$$

where $q = (q_1, q_2)$ and $\dot{q} = (\dot{q}_1, \dot{q}_2)$ are respectively position and velocity of the third body, q_a/q_b and m_a/m_b are respectively positions and masses of the revolving bodies, $V(q) = \frac{1-\mu}{\|q-q_a\|} + \frac{\mu}{\|q-q_b\|}$, $r(t) = \frac{c^2}{1+e \cos(\vartheta(t))}$, e is the eccentricity of the ellipse, ϑ is the true anomaly, $c = a(1 - e^2)$ (a is the major semi-axis of the ellipse), G is the gravitational constant, $M = m_a + m_b$ and $\mu = \frac{m_a}{M}$, $\|\cdot\|$ represents the Euclidean norm, $\mathbb{E}_{2n} = \begin{pmatrix} \mathbb{O}_n & \mathbb{I}_n \\ -\mathbb{I}_n & \mathbb{O}_n \end{pmatrix}$.

To find out more about the construction of (1.1) and for a comprehensive study of the ERTBP in accordance with a Lagrangian approach, refer to [10].

1.1 Hamiltonian function

Performing the Legendre transform on (1.1) the velocity, expressed in function of position and conjugate momenta, results $\dot{q}_i = \frac{p_i}{r^2(t)} \pm \frac{c\sqrt{GM} q_i}{r^2(t)}$ so the

Hamiltonian function obtained is

$$K(q_1, q_2, p_1, p_2, t) = \frac{1}{r^2(t)} \left(\frac{1}{2}(p_1^2 + p_2^2) + c\sqrt{GM}(p_1q_2 - q_1p_2) + \frac{1}{2}(q_1^2 + q_2^2) (c^2GM - r(t)GM) + r(t)GM V(q_1, q_2) \right) \quad (1.2)$$

$$\text{where } V(q_1, q_2) = \frac{1-\mu}{\sqrt{(q_1-\mu)^2+q_2^2}} + \frac{\mu}{\sqrt{(q_1-1+\mu)^2+q_2^2}}.$$

Proposition 1. The solutions of (1.2) with independent variable t are the same solutions of the Hamiltonian

$$H(q_1, q_2, p_1, p_2, \vartheta) = \frac{1}{2}(p_1^2 + p_2^2) + p_1q_2 - q_1p_2 + \frac{e \cos(\vartheta)}{2(1 + e \cos(\vartheta))} (q_1^2 + q_2^2) + \frac{1}{1 + e \cos(\vartheta)} V(q_1, q_2) \quad (1.3)$$

with independent variable θ .

Proof. It is clearly seen that (1.2) can be written in the form

$$K(q_1, q_2, p_1, p_2, t) = \frac{c\sqrt{GM}}{r^2(t)} \bar{K}(q_1, q_2, p_1, p_2, t) \quad (1.4)$$

where

$$\bar{K}(q_1, q_2, p_1, p_2, t) = \frac{1}{2c\sqrt{GM}}(p_1^2 + p_2^2) + p_1q_2 - q_1p_2 + \frac{1}{2}(q_1^2 + q_2^2) \left(c\sqrt{GM} - \frac{c\sqrt{GM}}{1 + e \cos(\vartheta(t))} \right) + \frac{c\sqrt{GM}}{1 + e \cos(\vartheta(t))} V(q_1, q_2) \quad (1.5)$$

and using $r^2(t) = \frac{c\sqrt{GM}}{\vartheta(t)}$ in (1.4), we obtain

$$K(q_1, q_2, p_1, p_2, t) = \vartheta(t) \bar{K}(q_1, q_2, p_1, p_2, t), \quad (1.6)$$

where $\dot{\vartheta}(t) > 0$, and so the change of variable $t \rightarrow \vartheta(t)$ is a diffeomorphism. The Hamilton equations of (1.6) are in the form

$$\dot{q}_i = \vartheta \frac{d\bar{K}}{dp_i}, \quad \dot{p}_i = -\vartheta \frac{d\bar{K}}{dq_i} \quad (1.7)$$

and, considering ϑ as independent variable, we have also

$$\dot{q}_i = \frac{dq_i}{d\vartheta} \frac{d\vartheta}{dt} = \frac{dq_i}{d\vartheta} \dot{\vartheta} \quad , \quad \dot{p}_i = \frac{dp_i}{d\vartheta} \frac{d\vartheta}{dt} = \frac{dp_i}{d\vartheta} \dot{\vartheta} . \quad (1.8)$$

Equating both expressions (1.7) and (1.8), we obtain

$$\frac{dq_i}{d\vartheta} = \frac{d\bar{K}}{dp_i} \quad , \quad \frac{dp_i}{d\vartheta} = -\frac{d\bar{K}}{dq_i}$$

With the rescaling $(q_i, p_i) \rightarrow (q_i, c\sqrt{GM}p_i)$ we arrive to the Hamiltonian function (1.3), that is clearly 2π -periodic due to dependency of ϑ only by the cosine function. \square

1.1.1 Hamiltonian vector field

It is known that the system defined by the Hamiltonian (1.3) has five equilibrium points (the collinear L_1, L_2, L_3 and the equilateral L_4, L_5) and that they are the same equilibrium points of the Circular Restricted case.

In this thesis we are interested in the study of the equilateral points, and, due to their symmetry, we choose to study L_4 , which correspond to the point

$$L_4 = \left(\frac{1}{2} - \mu, \frac{\sqrt{3}}{2}, -\frac{\sqrt{3}}{2}, \frac{1}{2} - \mu \right).$$

The Hamiltonian vector field relative to the Hamiltonian (1.3) is by definition $X_H = \mathbb{E}_4 \nabla H$, so its linearization around L_4 results in the form $DX_H = \mathbb{E}_4 H''$, where H'' is the Hessian of H calculated in L_4 . Through a canonical transformation it is possible to translate L_4 in the origin, so the linearization $(DX_H)|_{(0,0,0,0)}$ can be write as

$$A_{\mu,e}(\vartheta) = \begin{pmatrix} 0 & 1 & 1 & 0 \\ -1 & 0 & 0 & 1 \\ -\frac{1}{4(1+e\cos(\vartheta))} - \frac{e\cos(\vartheta)}{1+e\cos(\vartheta)} & -\frac{3\sqrt{3}(2\mu-1)}{4(1+e\cos(\vartheta))} & 0 & 1 \\ -\frac{3\sqrt{3}(2\mu-1)}{4(1+e\cos(\vartheta))} & \frac{5}{4(1+e\cos(\vartheta))} - \frac{e\cos(\vartheta)}{1+e\cos(\vartheta)} & -1 & 0 \end{pmatrix} . \quad (1.9)$$

Note that the matrix (1.9) depends on ϑ and that it is parametric through μ and e .

1.2 Extended phase space

For what we have just said, L_4 is an equilibrium of a system of four periodic ϑ -dependent differential equations, but we can read them as periodic solutions of a system of five autonomous differential equations in the extended phase space. Then, through the Poincaré theory, we can study the stability of the periodic orbit as the stability of the associated fixed point on a Poincaré map.

If we call P the Poincaré map and \bar{y} its fixed point, a version of the Lyapunov spectral theorem establishes that if at least one of the eigenvalues of $DP(\bar{y})$ is in absolute value greater than 1 then \bar{y} is instable, and if all the eigenvalues of $DP(\bar{y})$ are in absolute value smaller than 1 then \bar{y} is asymptotically stable. So what we have to do now is to find how to get the spectrum of the linearization of a Poincaré map.

To achieve our purpose we have first to define the monodromy matrix of a periodic orbit and its connection with the Poincaré map.

Definition 1. Let us consider a hamiltonian vector field X , Φ_t^X its flow at time t , γ a 2π -periodic orbit and $\bar{y} \in \gamma$. The matrix

$$M = D\Phi_{2\pi}^X(\bar{y}) \quad (1.10)$$

is called the monodromy matrix of γ .

The matrix $D\Phi_t^X(y)$ satisfies, $\forall y$ and $\forall t$, the variational equation

$$\frac{d}{dt} D\Phi_t^X(y) = DX(\Phi_t^X(y)) D\Phi_t^X(y)$$

with the initial condition $D\Phi_0^X = \mathbb{I}$ (because Φ_0^X is the identity function). So the monodromy matrix M of a 2π -periodic orbit is the solution, evaluated in 2π , of the differential equation

$$\dot{M} = DX(\Phi_t^X(y)) M \quad , \quad M(0) = \mathbb{I}. \quad (1.11)$$

The following Proposition give us the relation between the eigenvalues of the monodromy matrix and the eigenvalues of the linearization of its correlated Poincaré map.

Proposition 2. Let us consider an hamiltonian vector field X , Φ_t^X its flow at time t , γ a 2π -periodic orbit and $\bar{y} \in \gamma$. Let us also consider the monodromy

matrix M and the linearization of the Poincaré map $DP(\bar{y})$. Then

$$\sigma(M) = \sigma(DP(\bar{y})) \cup \{1\} \quad (1.12)$$

where $\sigma(A)$ indicates the set of all eigenvalues of the matrix A .

Proof. Refer to [7]. □

Returning to our problem, by using in (1.11) that $\Phi_t^{X_H}(\bar{y}) = L_4 \forall t$ and that $(DX_H)|_{L_4}(\vartheta)$ is the matrix defined in (1.9), the monodromy matrix of the periodic orbit associated to L_4 is the solution $M(2\pi)$ of the system

$$\dot{M} = A_{\mu,e}(\vartheta) M \quad , \quad M(0) = \mathbb{I}_4. \quad (1.13)$$

As the system is Hamiltonian, it is known that the monodromy matrix is a symplectic matrix, and therefore it is known that if λ is an eigenvalue of M also $\frac{1}{\lambda}, \bar{\lambda}, \frac{1}{\bar{\lambda}}$ are. Using this characterization of the spectrum of M together with (1.12), for the previously mentioned Lyapunov spectral theorem we can conclude that we have linear stability if all the eigenvalues of M are in absolute value equal to 1.

Thus, to determine the region of linear stability of L_4 we can apply the following algorithm: $\bar{\mu}$ and \bar{e} are fixed on the parameter plane and then the monodromy matrix is calculated numerically using (1.13); the couple $(\bar{\mu}, \bar{e})$ is considered to represent a parametric configuration of linear stability if all the eigenvalues of M are in absolute value equal to 1. Iterating this algorithm for different points on the parameter plane, the linear stability region for L_4 in the ERTBP appears as the black dotted area in Figure 1.1.

1.3 Hamiltonian vector field with E-property

In this section we explain how to halve the integration period of (1.13). We start defining a useful property for system of differential equations, called the *E-property*, described by Hale in [3] and then we show how to take advantage of this property in our problem, retracing the work of Meire and Vanderbauwhedein (see [6]).

Definition 2. A system of n differential equations $\dot{Y} = A(t)Y$ is said to have *property E with respect to S* if there exists a symmetric, constant matrix S of order n such that $S^2 = \mathbb{I}_n$ and

$$A(-t) = -S A(t) S .$$

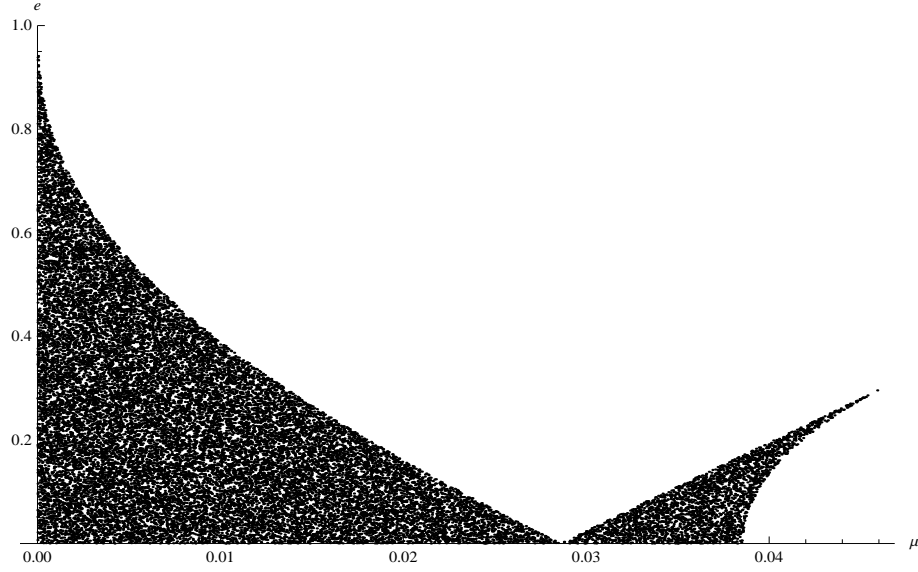


Figure 1.1: graphic elaboration in `Mathematica 8` of `Fortran 90` numerical results (see Chapter 3). The black dotted area indicates the linear stability region for L_4 in the ERTBP.

This property was described for systems of differential equations, and, considering a system that is T -periodic, it can be improved as follows

Proposition 3. Let us consider a system of differential equation $\dot{Y} = A(t)Y$, where Y and A are $n \times n$ matrices and A is T -periodic and continuous in t , and let us also assume that this system has the *property E with respect a matrix S* for a fixed matrix S . Then

$$Y(t) = S Y(-t) S \quad \forall t \in \mathbb{R} \quad (1.14)$$

and

$$Y(T) = S Y\left(\frac{T}{2}\right)^{-1} S Y\left(\frac{T}{2}\right) \quad (1.15)$$

where Y is a fundamental matrix of $\dot{Y} = A(t)Y$ satisfying $Y(0) = \mathbb{I}_n$.

Proof. Note first that if $Y(t)$ is a solution of $\dot{Y} = A(t)Y$ also $SY(-t)$ is: $(SY(-t))' = -S\dot{Y}(-t) = -S(A(-t)Y(-t))$ as so we have that $\dot{Y}(-t) = (-S^{-1})(-SA(-t)Y(-t)) = A(-t)Y(-t)$; with the same process it can be shown that also $SY(-t)S$ is a solution of $\dot{Y} = A(t)Y$.

Since $(SY(-t)S)|_{t=0} = S\mathbb{I}_n S = S^2 = \mathbb{I}_n$ and $Y(t)|_{t=0} = \mathbb{I}_n$, we have prove that $Y(t)$ and $SY(-t)S$ are two solutions of the same equation with the

same initial condition and so (1.14) is proved.

Setting $t = -\frac{1}{2}T$ in (1.14) and remembering, by the property of periodic systems, that $Y(t+T) = Y(t)Y(T)$, we obtain directly by substitution (1.15). \square

The system in (1.13) does not have the *E-property*, but acting as explained below we can overcome this lack. The following Proposition, that explains how achieve our purpose, presents the Hamiltonian version of the Lagrangian transformation theorized by Szebehely in [8].

Proposition 4. Let us fix a φ such that it solves $\sin(2\varphi) = \sqrt{3}(1-2\mu)\cos(2\varphi)$. Performing on (1.3) the canonical transformation

$$\begin{cases} \tilde{q} = Aq \\ \tilde{p} = A^{-T}p \end{cases} \quad \text{where } A = \begin{pmatrix} \cos(\varphi) & -\sin(\varphi) \\ \sin(\varphi) & \cos(\varphi) \end{pmatrix}.$$

the vector field of the Hamiltonian function that is obtained, linearized around \tilde{L}_4 (that is the equivalent of L_4 in the new coordinate system) is represented by the matrix

$$B_{\mu,e}(\vartheta) = \begin{pmatrix} 0 & 1 & 1 & 0 \\ -1 & 0 & 0 & 1 \\ -\frac{2e\cos(\vartheta)+3\sqrt{3(\mu-1)\mu+1}-1}{2e\cos(\vartheta)+2} & 0 & 0 & 1 \\ 0 & -\frac{2e\cos(\vartheta)-3\sqrt{3(\mu-1)\mu+1}-1}{2e\cos(\vartheta)+2} & -1 & 0 \end{pmatrix}. \quad (1.16)$$

Matrices (1.16) and (1.9) represent the linearization of two Hamiltonian functions related by a canonical transformation, so we can use (1.16) instead of (1.9) for the calculation of the monodromy matrix, and the relation (1.13) becomes

$$\dot{M} = B_{\mu,e}(\vartheta)M \quad , \quad M(0) = \mathbb{I}_4. \quad (1.17)$$

The advantage of (1.16) is that it has the *property E with respect to*

$$S = \begin{pmatrix} 1 & 0 & 0 & 0 \\ 0 & -1 & 0 & 0 \\ 0 & 0 & -1 & 0 \\ 0 & 0 & 0 & 1 \end{pmatrix}, \quad (1.18)$$

and this allow us to integrate the equation (1.17) until π instead of 2π , and to derive the monodromy matrix simply via (1.15), halving the computational

time. We come back numerically on this point in Chapter 3.

The region of linear stability for L_4 which is delineated by using the *E-property*-way is obviously the same as found in the preceding section (and shown in Figure 1.1).

Chapter 2

Bounding the stability region

In this chapter we analyze an alternative less-known approach to our problem, starting from the Lagrangian¹ formulation of the ERTBP. In the first part we retrace the work of Tschauner (see ([9])) showing how to separate the Lagrangian fourth-order system in two independent second-order systems. In the second part we exploit this separation theory together with the *E-property*, presented in the previous chapter, in order to define some boundaries for the stability region of L_4 on the parameter plane μ - e , as shown by Meire in [5].

2.1 Separation of the fourth-order system

As mentioned, we start from the Lagrangian formulation of the problem. By making with a Lagrangian approach what we have done in the Hamiltonian case in the first Chapter, the linearization in L_4 of the Lagrangian vector field that derives is

$$\begin{pmatrix} \dot{q} \\ \dot{v} \end{pmatrix} = \begin{pmatrix} \mathbb{O}_2 & \mathbb{I}_2 \\ r(\vartheta)C & 2\mathbb{E}_2 \end{pmatrix} \begin{pmatrix} q \\ v \end{pmatrix}, \quad (2.1)$$

where $C = \begin{pmatrix} c_1 & 0 \\ 0 & c_2 \end{pmatrix}$ has components $c_1 = \frac{3}{2} \left(1 + \sqrt{3(\mu-1)\mu+1} \right)$ and $c_2 = \frac{3}{2} \left(1 - \sqrt{3(\mu-1)\mu+1} \right)$, and $r(t) = \frac{1}{1+e \cos(\vartheta)}$.

¹We also tried to recreate all the theories presented in this chapter from the Hamiltonian point of view, but without success, because of their strong Lagrangian foundation. This does not mean that it is impossible to overcome this difficulty.

Proposition 5. Assume

$$g(\mu, e) = \frac{e^4}{3(\mu - 1)\mu + 1} + 2e^2 + 27(\mu - 1)\mu + 1 > 0. \quad (2.2)$$

Performing the θ -dependent transformation

$$\begin{pmatrix} q \\ v \end{pmatrix} = \begin{pmatrix} \mathbb{I}_2 & \mathbb{I}_2 \\ P_{\mu,e}^+(\vartheta) & P_{\mu,e}^-(\vartheta) \end{pmatrix} \begin{pmatrix} \eta \\ \xi \end{pmatrix}, \quad (2.3)$$

where

$$P_{\mu,e}^\pm(\vartheta) = r(\vartheta) \begin{pmatrix} p_{11} & p_{12}^\pm \\ p_{21}^\pm & p_{22} \end{pmatrix} \quad (2.4)$$

with

$$\begin{aligned} p_{11} &= -\frac{e}{2} \sin(\vartheta) - \frac{3e^2}{4(c_2 - c_1)} \sin(2\vartheta) \\ p_{12}^\pm &= \left(h_2^\pm + e \cos(\vartheta) - \frac{3e^2}{4(c_2 - c_1)} \cos(2\vartheta) \right) \\ p_{21}^\pm &= -\left(h_1^\pm + e \cos(\vartheta) + \frac{3e^2}{4(c_2 - c_1)} \cos(2\vartheta) \right) \\ p_{22} &= -\frac{e}{2} \sin(\vartheta) + \frac{3e^2}{4(c_2 - c_1)} \sin(2\vartheta) \end{aligned}$$

c_1 and c_2 defined as in (2.1) and $h_i^\pm = \frac{1}{4}(2c_i + 1 \mp \sqrt{g(\mu, e)})$, (2.1) becomes

$$\begin{pmatrix} \dot{\eta} \\ \dot{\xi} \end{pmatrix} = \begin{pmatrix} P_{\mu,e}^+(\vartheta) & \mathbb{O}_2 \\ \mathbb{O}_2 & P_{\mu,e}^-(\vartheta) \end{pmatrix} \begin{pmatrix} \eta \\ \xi \end{pmatrix} \quad (2.5)$$

Note: to make the notation easier to follow, henceforth in this Chapter we use $P_\pm(\vartheta)$ instead of $P_{\mu,e}^\pm(\vartheta)$. This does not remove the fact that the matrices $P_\pm(\vartheta)$ are still parametric.

Proof. First of all we have to verify that the transformation (2.3) is invertible, that is

$$\det \begin{pmatrix} \mathbb{I}_2 & \mathbb{I}_2 \\ P_+(\vartheta) & P_-(\vartheta) \end{pmatrix} \neq 0$$

i.e. the four columns of the matrix

$$\begin{pmatrix} 1 & 0 & 1 & 0 \\ 0 & 1 & 0 & 1 \\ r(\vartheta) p_{11} & r(\vartheta) p_{12}^+ & r(\vartheta) p_{11} & r(\vartheta) p_{12}^- \\ r(\vartheta) p_{21}^+ & r(\vartheta) p_{22} & r(\vartheta) p_{21}^- & r(\vartheta) p_{22} \end{pmatrix}$$

must be linearly independent. This is equivalent to impose

$$r^2(\vartheta) \det \begin{pmatrix} p_{11} & p_{11} \\ p_{21}^+ & p_{21}^- \end{pmatrix} \quad \text{and} \quad r^2(\vartheta) \det \begin{pmatrix} p_{12}^+ & p_{12}^- \\ p_{22} & p_{22} \end{pmatrix}$$

and the condition that results is $g(\mu, e) \neq 0$, as assumed.

Applying the transformation (2.3) to (2.1) we obtain the system

$$\begin{pmatrix} \dot{\eta} \\ \dot{\xi} \end{pmatrix} = (P_+ - P_-)^{-1} \begin{pmatrix} W_{11} & W_{12} \\ W_{21} & W_{22} \end{pmatrix} \begin{pmatrix} \eta \\ \xi \end{pmatrix} \quad (2.6)$$

where

$$\begin{aligned} W_{11} &= 2\mathbb{E}_2 P_+ - P_- P_+ + r(\vartheta) C - P'_+ \\ W_{12} &= -P_-^2 + 2\mathbb{E}_2 P_- + r(\vartheta) C - P'_- \\ W_{21} &= P_+^2 - 2\mathbb{E}_2 P_+ - r(\vartheta) C + P'_+ \\ W_{22} &= -2\mathbb{E}_2 P_- + P_+ P_- - r(\vartheta) C + P'_- . \end{aligned}$$

Requiring that the anti-diagonal elements of the 4x4 matrix in (2.6) are the null 2x2 matrix, i.e. imposing $W_{12} = \mathbb{O}_2$ and $W_{21} = \mathbb{O}_2$, we obtain

$$\begin{cases} P'_- = -P_-^2 + 2\mathbb{E}P_- + r(\vartheta) C \\ P'_+ = -P_+^2 + 2\mathbb{E}P_+ + r(\vartheta) C \end{cases} \quad (2.7)$$

and, using these conditions in order to simplify W_{11} and W_{22} , (2.6) becomes

$$\begin{pmatrix} \dot{\eta} \\ \dot{\xi} \end{pmatrix} = (P_+ - P_-)^{-1} \begin{pmatrix} P_+^2 + P_- P_+ & \mathbb{O}_2 \\ \mathbb{O}_2 & P_- P_+ - P_-^2 \end{pmatrix} \begin{pmatrix} \eta \\ \xi \end{pmatrix}$$

that is clearly equivalent to (2.5).

Now it remains to be proved that $P_{\pm}(\vartheta)$, as defined in (2.4), are solutions of the Riccati equations (2.7), but it is easy to verify by substitution. \square

Note that we have just shown that the transformation (2.3), with $P_{\pm}(\vartheta)$ as in (2.4), realizes (2.5), but not the reason why (2.4) should be in that form: for a constructive proof of $P_{\pm}(\vartheta)$ refer to [9].

So we can split the 4x4 system (2.1) in two independent 2x2 systems

$$\dot{\eta} = P_+(\vartheta) \eta \quad \dot{\xi} = P_-(\vartheta) \xi \quad (2.8)$$

where $P_{\pm}(\vartheta)$ are defined as in (2.4).

It is easy to verify that both systems in (2.8) are 2π -periodic and that they have the *property E with respect to S*, with $S = \begin{pmatrix} 1 & 0 \\ 0 & -1 \end{pmatrix}$.

Now it is clearly possible to perform Floquet theory, similar to what we did in the previous Chapter with the Hamiltonian vector field, separately on both systems in (2.8). What we do instead, is to explore a different approach to the investigation of the stability region of L_4 , which is tied directly to the separation theory just discussed.

2.2 Transition curves

In this section we discuss the existence of the transition curves, where with ‘transition curve’ we mean a curve that separates the region of linear stability from the region of instability of L_4 on the plane μ - e .

As can be seen in Figure 2.1, in the parametric region of which we are inte-

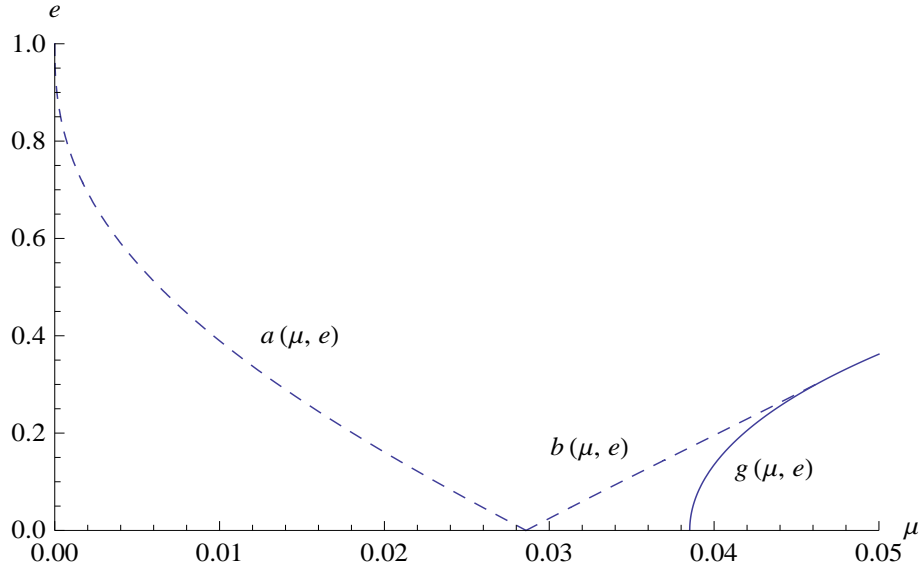


Figure 2.1: transition curves on the parameter plane.

rested we can note three different transition curves, and we call them $a(\mu, e)$, $b(\mu, e)$ and $g(\mu, e)$. As said by Tschauner in [9], $g(\mu, e)$ is the only analytical transition curve we can find on the parameter plane, and its existence is directly related to the separation theory presented in the previous section: $g(\mu, e)$, in fact, is the curve already defined in (2.2). What interests us is that many other transition curves, including $a(\mu, e)$ and $b(\mu, e)$, can be found numerically following the theory proposed by Meire (refer to [5]), and so what we do now is to retrace his work.

Note that in this section, for our convenience, we base all the discussion on the system

$$\dot{Y} = P_+(\vartheta)Y \quad , \quad Y(0) = \mathbb{I}_2 \quad (2.9)$$

but everything we say holds true for $\dot{Y} = P_-(\vartheta)Y$.

We start considering the following Lemma, that there will soon be useful.

Lemma 1. Let us consider the system (2.9), then its monodromy matrix is

in the form

$$M = \begin{pmatrix} \alpha & \beta \\ \gamma & \alpha \end{pmatrix}. \quad (2.10)$$

Proof. Calling $Y(\vartheta)$ the fundamental matrix of (2.9), we define the monodromy matrix as $M = Y(2\pi) = \begin{pmatrix} \alpha_1 & \beta \\ \gamma & \alpha_2 \end{pmatrix}$. As already said, (2.9) has the *E-property with respect to* $S = \begin{pmatrix} 1 & 0 \\ 0 & -1 \end{pmatrix}$ and so, using (1.15) with

$$Y(\pi) = \begin{pmatrix} y_{11} & y_{12} \\ y_{21} & y_{22} \end{pmatrix}, \quad (2.11)$$

we have to solve

$$\begin{pmatrix} \alpha_1 & \beta \\ \gamma & \alpha_2 \end{pmatrix} = \begin{pmatrix} 1 & 0 \\ 0 & -1 \end{pmatrix} \begin{pmatrix} y_{11} & y_{12} \\ y_{21} & y_{22} \end{pmatrix}^{-1} \begin{pmatrix} 1 & 0 \\ 0 & -1 \end{pmatrix} \begin{pmatrix} y_{11} & y_{12} \\ y_{21} & y_{22} \end{pmatrix}. \quad (2.12)$$

What results is

$$\alpha_1 = \alpha_2 = \frac{y_{11} y_{22} + y_{12} y_{21}}{y_{11} y_{22} - y_{12} y_{21}} \quad (2.13)$$

$$\beta = \frac{2 y_{22} y_{12}}{y_{11} y_{22} - y_{12} y_{21}} \quad (2.14)$$

$$\gamma = \frac{2 y_{11} y_{21}}{y_{11} y_{22} - y_{12} y_{21}} \quad (2.15)$$

and calling $\alpha = \alpha_1 = \alpha_2$ we obtain (2.10). \square

As said by Meire in [5], along the transition curves the eigenvalues of M are both equal to 1 or -1 , and using this property, together with the previous Lemma, we get to state the following Proposition.

Proposition 6. Let us consider the systems in (2.9) with $Y(\vartheta)$ as fundamental matrix. If the matrix $P_+(\vartheta)$, defined as in (2.4), takes parameter values on a transition curve, then at least one of the components of $Y(\pi)$ is equal to zero.

Proof. Knowing that $\det(Y(2\pi)) = 1$ and that along the transition curves $\sigma(Y(2\pi)) = \pm\{1, 1\}$, we get to set the system

$$\begin{cases} \alpha^2 - \beta\gamma = 1 \\ (\alpha \pm 1)^2 - \beta\gamma = 0 \end{cases}$$

that give us the condition $\beta\gamma = 0$. Using the definition of β and γ as in (2.14) and (2.15), impose $\beta\gamma = 0$ means

$$\frac{4y_{22}y_{12}y_{11}y_{21}}{(y_{11}y_{22} - y_{12}y_{21})^2} = 0 \quad (2.16)$$

which is clearly equivalent to ask that at least one of the components of $Y(\pi)$ is zero.

Now if we impose $y_{11} = 0$ in (2.16), by (2.13), (2.14) and (2.15) we obtain that the monodromy matrix is in the form

$$\begin{pmatrix} -1 & \beta \\ 0 & -1 \end{pmatrix} \text{ with two eigenvalues } -1$$

and by imposing $y_{22} = 0$ we obtain

$$\begin{pmatrix} -1 & 0 \\ \gamma & -1 \end{pmatrix} \text{ still with two eigenvalues } -1.$$

In the same way, by imposing $y_{12} = 0$ or $y_{21} = 0$ we obtain

$$\begin{pmatrix} 1 & \beta \\ 0 & 1 \end{pmatrix} \text{ or } \begin{pmatrix} 1 & 0 \\ \gamma & 1 \end{pmatrix}, \text{ both matrices with two eigenvalues } 1.$$

So, the choice of which component to make 0 in (2.16) identifies a different transition curve on the parameter plane μ - e . \square

What we have to do now is, therefore, to find which particular components of (2.11) are associated to the transition curves of our interest $a(\mu, e)$ and $b(\mu, e)$: for this refer to the Subsection 3.2.1 of the next Chapter.

The numerical advantage of this approach is obvious: it allows us to investigate the parametric stability of L_4 simply integrating until π both systems in (2.8) and searching for the zeros among the components of their solutions, without computing eigenvalues as done with the previous methods.

Chapter 3

Numerical results

In the two previous Chapters we discussed theoretically different approaches to the investigation of the stability of L_4 , all applicants the integration of some differential equations. In this final part we want to present and discuss some of our main numerical results and compare them with those that were obtained from Danby and Meire (see [2] and [5]).

3.1 Algorithms

The main numerical operation to be performed is certainly the integration of matrix differential equations in the form

$$\dot{Y} = R_{\mu,e}(\vartheta) Y \quad , \quad Y(0) = \mathbb{I}_4, \quad (3.1)$$

where the 4x4 parametric matrix $R_{\mu,e}(\vartheta)$ corresponds to:

- $A_{\mu,e}(\vartheta)$ as in (1.13), associated to the Hamiltonian vector field, or
- $B_{\mu,e}(\vartheta)$ as in (1.17), associated to the Hamiltonian vector field with the *E-property*, or
- $P_{\mu,e}(\vartheta)$ as in (2.5), the block diagonal matrix which derives from Tschauner's theory presented in the second Chapter.

The first numerical result that we want to achieve is, of course, the determination of the linear stability of L_4 on the parameters plane μ - e ; to do this we must first decide which algorithm to work, which integration step to use and which error tolerance to esteem.

We consider the explicit Runge-Kutta algorithms of order 4, 8 and 12 and

we map the subset of the parameter plane defined by $[0, 0.05] \times [0, 1]^1$ with a grid of 100 equispaced points: we search for an integration step for which the error made (compared to the maximum modulus of the components of the solution) is $\sim 10^{-8}$. By implementing those three algorithms in Fortran 90 we obtain the results shown in Table 3.1.

| | | | | | | | | |
|--|--------------------|-------------------|--|--------------------|-------------------|---|-------------------|-------------------|
| $\dot{Y} = R_{\mu,e}(\vartheta) Y \quad , \quad Y(0) = \mathbb{I}_4$ | | | | | | | | |
| integrating untill 2π | | | integrating untill π (with <i>property E</i>) | | | | | |
| $R_{\mu,e}(\vartheta) = A_{\mu,e}(\vartheta)$ | | | $R_{\mu,e}(\vartheta) = B_{\mu,e}(\vartheta)$ | | | $R_{\mu,e}(\vartheta) = P_{\mu,e}(\vartheta)$ | | |
| RK4 | RK8 | RK12 | RK4 | RK8 | RK12 | RK4 | RK8 | RK12 |
| $\frac{2\pi}{5000}$ | $\frac{2\pi}{200}$ | $\frac{2\pi}{40}$ | $\frac{2\pi}{3900}$ | $\frac{2\pi}{128}$ | $\frac{2\pi}{32}$ | $\frac{2\pi}{530}$ | $\frac{2\pi}{25}$ | $\frac{2\pi}{12}$ |
| 698s | 123s | 42s | 223s | 31s | 14s | 293s | 40s | 26s |

Table 3.1: comparison of algorithms on the three different differential systems in study. The second last row shows the integration step that should be used for each system and each algorithm for having an mean error on the matrix $\sim 10^{-8}$. The last row shows the computational time that was needed for 100 points in each case by running the algorithms on an Intel Pentium Dual Core E2160 (1.8 GHz).

As we expected, we can immediately see that, whatever the algorithm used, the integration of (3.1) with (1.17) untill π requires less computational time compared to integrating with (1.13) untill 2π ; however, what was less expected according to the theory, is that the saving time is greater than 50%: this is due to the fact that, in addition to integrate over one half period, we can use a less-fine discretization. Regarding the integration with (2.5) we can say that it would be convenient because of its convergence for larger integration steps, except that the higher number of evaluations of the parameters to be carried out worsens the computational time.

3.2 Stability region in the μ - e plane

So, according to the results presented in Table 3.1, we decide to integrate the system (3.1) with $R_{\mu,e}(\vartheta) = B_{\mu,e}(\vartheta)$ using the explicit Runge-Kutta of order

¹It is known (see for example [2]) that the stability region for L_4 in the ERTBP is certainly for values of μ in the range $0 \leq \mu \leq 0.05$, so there is no interest in investigating out of these intervals.

12. The results of this numerical work has already been shown in Figure 1.1.

3.2.1 Numerical and analytical boundaries

Now we treat the alternative approach set out in the second Chapter: we show how the curve $g(\mu, e) = 0$ (as defined in (2.2)) appears to be a transition curve

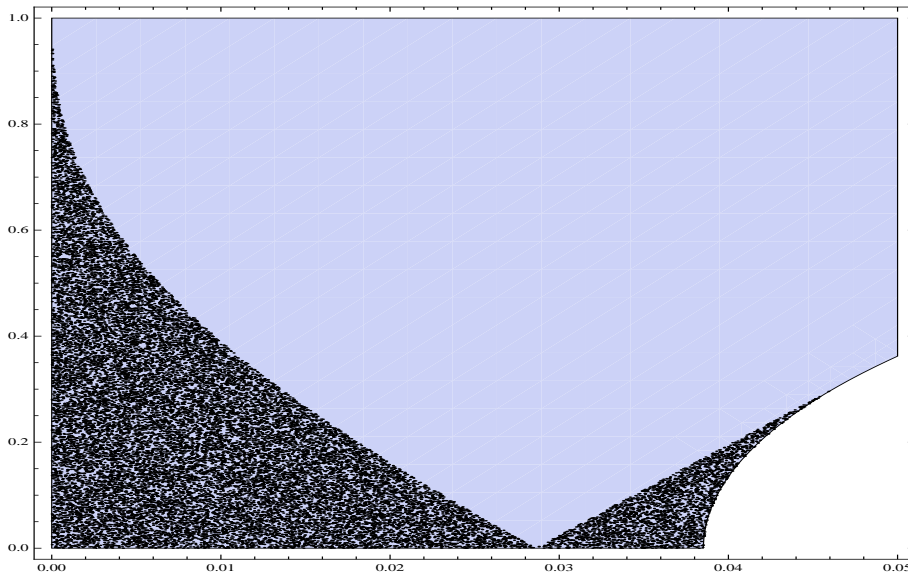


Figure 3.1: graphic elaboration in `Mathematica 8` of `Fortran 90` numerical results. The black dotted area indicates the linear stability region for L_4 in the ERTBP, the shaded area represents the subset of the plane μ - e for which the condition (2.2) is satisfied.

and we illustrate the numerical results obtained by the implementation of the algorithm for the search of other transition curves, as explained in Section 2.2.

In Figure 3.1 is indicated, as a shaded area, the subset of the plane of the parameters that satisfies the condition $g(\mu, e) > 0$ (as requested in (2.2)) and from this we can deduce that the condition $g(\mu, e) = 0$ is a right edge for the area of stability. Due to our interest for values of μ and e in $[0, 0.05] \times [0, 1]$, we can explicit the condition $g(\mu, e) = 0$ as a function of μ , satisfying

$$e(\mu) = \sqrt{-3\mu^2 + 2\sqrt{6}\sqrt{-3\mu^4 + 6\mu^3 - 4\mu^2 + \mu} + 3\mu - 1}. \quad (3.2)$$

We can perform a simple test for verifying the goodness of this result: intersecting $e(\mu)$ with the axis $e = 0$ we find the point $(0.0385209, 0)$ that

corresponds to the well-known Routh value, i.e. the point $(\mu_{Routh}, 0)$ that represents the upper bound for the linear stability region of L_4 in the Circular Restricted Three-Body Problem.

Remembering that (3.2) is the only analytical transition curve that we can find, for the detection of other transition curves we operate as done by Meire ([5]): we integrate until π the system

$$\dot{Y} = P_{\mu,e}^+(\vartheta) Y \quad , \quad Y(0) = \mathbb{I}_2 \quad (3.3)$$

with $P_{\mu,e}^+(\vartheta)$ as defined in (2.4), and look for what values of μ and e it results that y_{11} or y_{22} (components of the matrix $Y(\pi)$ as in (2.11)) is equal to zero. Of course, we should also investigate what happens using $P_{\mu,e}^-(\vartheta)$ and see what kind of curves are generated imposing $y_{12} = 0$ and/or $y_{21} = 0$, but a

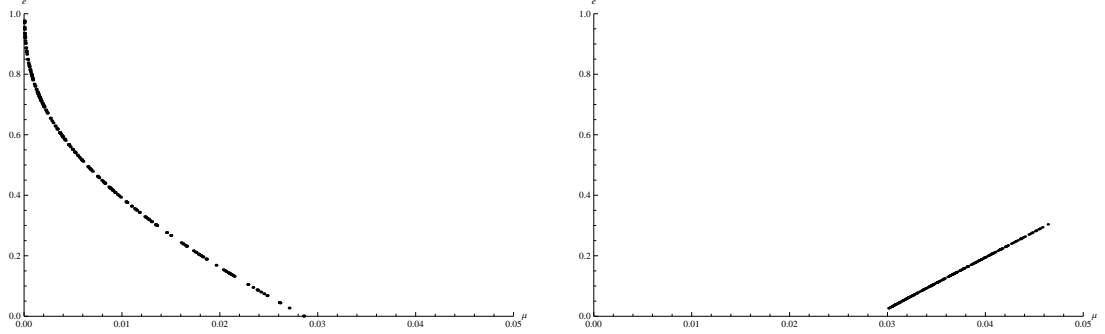


Figure 3.2: points on the parametric plane for which the component y_{11} (figure on the left) and y_{22} (figure on the right) of the solution of (3.3) are 0 with a numerical tolerance $\sim 10^{-7}$. It is clearly seen that using these two curves together with (3.2) we define the same stability region of Figure 1.1.

posteriori it is seen that all the information we need for circumscribing the stability region are related to $P_{\mu,e}^+(\vartheta)$. A graphic justification of what we have just said is given in Figure 3.2.

3.2.2 Right limit point

The stability region of L_4 , as shown in Figure 1.1, presents, in addition to the two intersections with the axis $\mu = 0$, three limit points: calling them Γ , Σ and Λ , they are identified in Figure 3.3. It is evident that the points Γ and Σ are related to the Circular Restricted problem, while point Λ is a peculiarity of the elliptical version. One who studied the stability, using his words, “in the sharp and thin cusp”, was Danby (see [2]) that has come to state the approximation $\Lambda = (0.04698, 0.3143)$: what we would do

in this part is just to improve this approximation. We can see Λ as the only point of intersection between the analytical curve $e(\mu)$ (defined as in (3.2)) and the numerical transition curve of the eigenvalues -1 (that is the one shown in Figure 3.2.2). In other words, we can define Λ as the only point on the analytical curve for which the monodromy matrix of the system $\dot{Y} = P_{\mu,e(\mu)}^+(\vartheta) Y$ has both the eigenvalues equal to -1 . By implementing this searching algorithm in `Fortran 90`, with arbitrary precision, we arrived in estimating Λ as the point

$$0.04699080701821065361786925, 0.3145071597549351412371152.$$

Note that in this case we integrated with a Runge-Kutta of order 4, because it is pointless to use higher order algorithms since to the slow convergence that all our three algorithms considered show in a neighborhood of Λ .

3.3 Reduced integration

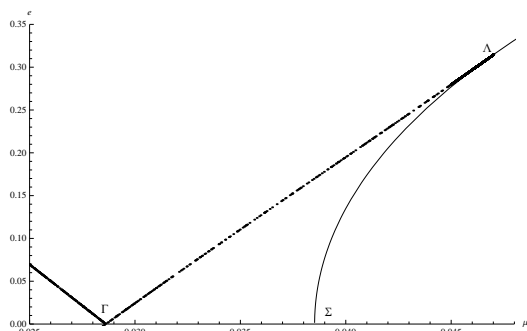


Figure 3.3: identification of the points of intersection between two of the transition curves and the analytical one.

Assuming that the transition curves useful for limiting the region of stability are related exclusively to the matrix $P_{\mu,e}^+(\vartheta)$ (as said in Subsection 3.2.1), we can reasonably believe that the region of stability itself is some way linked to $P_{\mu,e}^+(\vartheta)$. So we integrate the system (3.3) first with $P_{\mu,e}^+(\vartheta)$ and then with $P_{\mu,e}^-(\vartheta)$, and finally we compare the stability areas that their monodromy matrices define. What it results is shown in Figure 3.4 and confirms our expectations, and so we can affirm that the stability re-

gion defined integrating the fourth-order system

$$\dot{Y} = \begin{pmatrix} P_{\mu,e}^+(\vartheta) & \mathbb{O}_2 \\ \mathbb{O}_2 & P_{\mu,e}^-(\vartheta) \end{pmatrix} Y \quad , \quad Y(0) = \mathbb{I}_4 \quad (3.4)$$

is the same that can be found integrating the second-order system

$$\dot{Y} = P_{\mu,e}^+(\vartheta) Y \quad , \quad Y(0) = \mathbb{I}_2. \quad (3.5)$$

The advantage of this is clearly evident, in particular as regards the computational time, and Table 3.2 is an explanation of this.

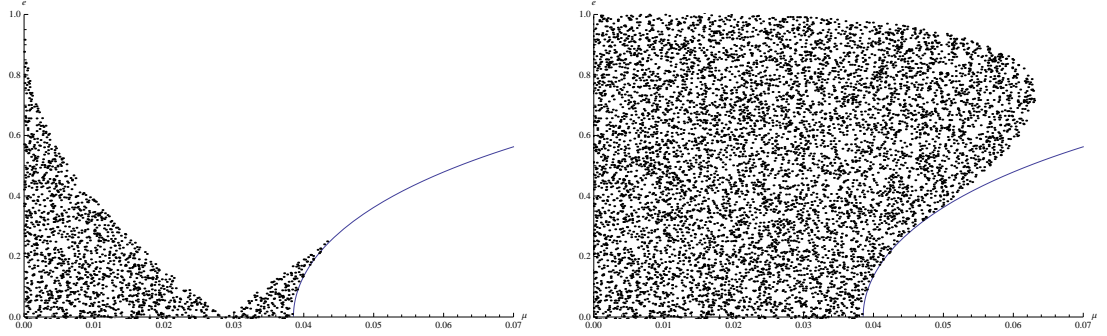


Figure 3.4: Every black dotted point represent a parametric configuration for which the monodromy matrix of (3.3) (generated with $P_{\mu,e}^+(\vartheta)$, in the left figure, and with $P_{\mu,e}^-(\vartheta)$ in the right one) has all eigenvalues in norm equal to 1. The curve drawn in both figures is the function (3.2).

| System (3.4) | | | System (3.5) | | |
|-------------------------|-----------------|-----------------|----------------|-----------------|-----------------|
| integrating until π | | | | | |
| RK4 | RK8 | RK12 | RK4 | RK8 | RK12 |
| $\sim 10^{-9}$ | $\sim 10^{-14}$ | $\sim 10^{-15}$ | $\sim 10^{-9}$ | $\sim 10^{-14}$ | $\sim 10^{-15}$ |
| 229s | 927s | 1504s | 118s | 502s | 843s |

Table 3.2: comparison of algorithms on a grid of 100 equispaced points on the parameter plane. The second last row shows the mean error made for each algorithm (compared to the maximum modulus of the components of the solution) using $\frac{2\pi}{1200}$ as integration step. The last row shows the computational time that was needed in each case.

It is not difficult to verify (numerically) that what has been said about $P_{\mu,e}^+(\vartheta)$ applies on the whole parameters plane and not only in the region $[0, 0.05] \times [0, 1]$ of which we have discussed.

Bibliography

- [1] K. T. Alfriend - R. H. Rand, *Stability of the Triangular Points in the Elliptic Restricted Problem of Three Bodies*, AIAA Journal, Volume 7.6, p1024, 1969.
- [2] J. M. A. Danby, *Stability of the Triangular Points in the Elliptic Restricted Problem of Three Bodies*, The Astronomical Journal, Volume 69.2, pp171-172, 1964.
- [3] J. K. Hale, *Ordinary differential equations*, Robert E. Krieger, p280, 1980.
- [4] A. P. Markeev, *On the stability of the triangular libration points in the elliptic restricted three-body problem*, PMM, 34, pp227-232, 1970.
- [5] R. Meire, *The stability of the triangular points in the elliptic restricted problem*, Celestial Mechanics, 23, pp89-95, 1981.
- [6] R. Meire - A. Vanderbauwhede, *A useful result for certain linear periodic ordinary differential equations*, Journal of Computational and Applied Mathematics, Elsevier B.V., pp59-61, 1979.
- [7] K. R. Meyer - G. R. Hall, *Introduction to the Hamiltonian Dynamical Systems and the N-Body Problem*, Springer-Verlag, 1992.
- [8] V. G. Szebehely, *Theory of Orbits*, Academic Press, 1967.
- [9] J. Tschauner, *Die Aufspaltung der Variationsgleichungen des Elliptischen Eingeschränkten Dreikörperproblems*, Celestial Mechanics, Volume 3.3, pp395-402, 1971.
- [10] M. Zanlorenzi, *Soluzioni triangolari nel problema ristretto ellittico dei 3 corpi*, Tesi di Laurea in Fisica, Università degli Studi di Padova, 2010.